EFFECT OF A MAGNETIC FIELD ON PERISTALTIC TRANSPORT OF BINGHAM PLASTIC FLUID IN A SYMMETRIC CHANNEL

Farah Alaa Adnan[a*], Ahmad M. Abdul Hadi[a]

[a] *Mathematics Department, College of Science, University of Baghdad., Iraq.*

**E- mail address:farrah.a_adnan@yahoo.com.*

ABSTRACT: *In this paper we address the effect of a magnetic field on peristaltic transpot of Bingham plastic fluid in a symmetric channel, and convective conditions of heat. Space dependent viscosity, Novel Soret and Dufour effects are taken into consideration. The formulation of the problem is presented through, the lubrication approach is used Impact of variables reflecting the features of wall properties, Biot numbers, Hartman number, Bingham number, Brinkman number, Schmidt number, Soret and Dufour numbers on the velocity, heat transformation, and concentration coefficient are mentioned. In addition, the trapping phenomenon is analyzed.*

Keyword: *Bingham plastic fluid, a magnetic field, variable viscosity,Soret number and Dufour number effects*

1. INTRODUCTION:

Peristaltic transport is a form of material transport induced by a progressive wave of contraction expansion along the length of distensible tube mixing and transporting the fluid in the direction of the wave propagation, this kind of phenomenon is termed as peristaltic. It plays an important role in transporting many physiological fluids in the body under different situations as urine transport from kidney to bladder, the movement of chyme in the gastrointestinal tracts, transport of spermatozoa in the ductus efferent`s of the male reproductive tract, the movement of ovum in the fallopian tube, swallowing of food through esophagus and the vasomation of small blood vessels , many modern mechanical devices have been designed on the principle of peristaltic pumping to transport the fluids without internal moving parts, for example the blood pump in the heart-lung machine and peristaltic transport of naxious fluid in unclear industry. As a result of its existence in various fields such as industry and physiology, peristalsis transport of non-Newtonian fluids received considerable attention in the past, since many analysis have been made for peristaltic mechanism with the consideration of both viscous and non-Newtonian fluids (see [1-7]). The non-Newtonian fluids deviate from the classical Newtonian linear relationship between the shear stress and shear rate, due to complex rheological properties it is difficult to suggest a single model which exhibits all properties of non-Newtonian fluids. Among the many suggested models of non-Newtonian fluids, Abd-Alla et al. [8] discussed the effect of a radial magnetic field on peristaltic transport of Jeffrey fluid in cylindrical geometry, Abd-Alla et al. [9] discussed the influence of rotation and initial stresses on the peristaltic flow of fourth grade fluid in an asymmetric channel, The peristaltic flow of nanofluid through a porous medium with mixed convection is analyzed by Nowar [10], Kothandapani et al. [11] studied the combined effects of radiation and magnetic field on peristaltic transport of nanofluid, Hayat et al. [12] explore the peristaltic flow of Bingham plastic fluid having a variable viscosity in asymmetric channel with the Soret and Dufour numbers accounted, and Alaa et al. [13] studied the effect of a magnetic field on peristaltic transport of Bingham plastic fluid in asymmetric channel. In the present study, we investigated the peristaltic transport of peristaltic transport of Bingham plastic fluid under the effect of a magnetic field, Soret and Dufour numbers through porous medium in in a symmetric channel and regular perturbation method is used. Series solutions for stream function, heat and concentration are given. The influence of the physical parameters of the problem are discussed and illustrated graphically.

2. Physical Model and Fundamental Equation:

The governing equation for the conservation of mass, momentum, energy and particles concentration for Bingham plastic fluid in a symmetric channel can be written as:

Equation of mass conservation

$$div\,\bar{U} = 0 \qquad (1)$$

Equation of momentum conservation

$$\rho\frac{d\,\bar{U}}{d\,\bar{t}} = div\,\bar{\tau} - \delta {B_0}^2\bar{U} - \frac{\mu(y)}{k_0}\bar{U} \qquad (2)$$

Equation of energy conservation

$$\rho c_p\frac{d\,\bar{T}}{d\,\bar{t}} = \kappa\nabla^2 T + \bar{S}.(grad\,\bar{U}) + \sigma {B_0}^2\bar{U} + \frac{DK_T}{C_s}\nabla^2 C \qquad (3)$$

Equation of particles concentration

$$\frac{dC}{d\bar{t}} = D\nabla^2 C + \frac{DK_T}{T_m}\nabla^2 T \qquad (4)$$

Where

$\nabla^2 = \frac{\partial^2}{\partial x^2} + \frac{\partial^2}{\partial y^2}$ Is the laplace operator.

Where $(\rho, \sigma, c_p, \kappa, K_T, D, T_m, and\ C_s)$denotes the fluid density, the electrical conductivity, the specific heat, and the thermal conductivity, thermal diffusion ratio, the coefficient of mass diffusivity, the mean temperature, and the concentration susceptibility respectively. Furthermore T and C are temperature and concentration of the material. While the velocity and the extra stress tensor of Bingham plastic fluid are

$$\bar{U} = (\bar{U}\ (\bar{X}\ ,\bar{Y}\ ,\ \bar{t}), \bar{V}(\bar{X}\ ,\bar{Y}\ ,\ \bar{t}), 0)$$

$$\bar{s} = \left(\mu(\bar{Y}) + \frac{\tau_y}{\dot{\gamma}}\right)\bar{A}_1, \text{For } \tau \geq \tau_y, \qquad (5)$$

$$\bar{s} = \bar{A}_1 = 0, \quad for\ \tau < \tau_y,$$

Where $\bar{s} = \begin{bmatrix} \bar{s}_{xx} & \bar{s}_{xy} \\ \bar{s}_{yx} & \bar{s}_{yy} \end{bmatrix}$; $\bar{\dot{\gamma}} = \frac{1}{\sqrt{2}}\sqrt{trac(\bar{A}_1)^2}$

And $\bar{A}_1$ $is\ the\ first\ \ Rivin - Ericksen\ tensor$ and $\tau_y$is the yield stress:

$$\bar{A}_1 = grad\,\bar{U} + (grad\,\bar{U})^T \qquad (6)$$

Now the Cauchy stress tensor denoted by $\bar{\tau}$ such that

$$\bar{\tau} = -\bar{P}\bar{I} + \bar{S} \qquad (7)$$

Where $\bar{P}$ the pressure, $\bar{I}$ the identity tensor and $\bar{S}$ the extra stress tensor for Bingham liquid.

3. Mathematical Modeling

Consider the peristaltic flow of an incompressible electrically conducting Bingham material in a symmetric channel having a total width of $d_1 + d_2$ (see fig.1). Let us consider $\bar{X}$ and $\bar{Y}$ axes along and vertical to the flow respectively. The velocity components $\bar{U}$ and $\bar{V}$ ly along $\bar{X}$ and $\bar{Y}$ directions respectively. There is no component in $\bar{Z}$ direction as shown in Fig. (1). Aspects of Joule heating is present. The material is electrically conducting via a magnetic field of strength B_0 is applied in transverse direction to the flow. The features of thermo-diffusion and diffusion-thermo effects are also accounted. For the channel wall comprises the convective cooling effects.

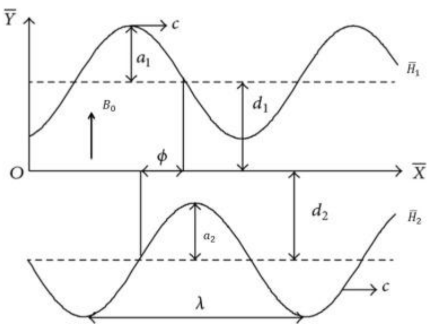

Fig. (1) Geometry of the problem

Channel waves propagating along the axial direction moving with constant speed c are represented by:

$\bar{H}_1(\bar{X}, t) = d_1 + a_1 sin\frac{2\pi}{\lambda}(\bar{X} - c\bar{t})$ Upper wall

$\bar{H}_2(\bar{X}, t) = -d_2 - a_2 \sin(\frac{2\pi}{\lambda}(\bar{X} - c\bar{t}) + \varphi)$Lower wall (8)

In which a_1, a_2 are the wave amplitudes, λ the wavelength and φ is the phase difference. Here phase difference φ lies between 0 to π. Moreover $\varphi = 0$ represents the symmetric channel with a wave out of phase and $\varphi = \pi$ represents wave which is in phase. And the following parameters a_1, a_2, d_1, d_2 and φ are satisfying the relation:

$$(d_1 + d_2)^2 \geq a_1{}^2 + a_2{}^2 + 2a_1 a_2 \cos\varphi \quad (9)$$

The continuity equation can be written as:

$$\frac{\partial \bar{U}}{\partial \bar{X}} + \frac{\partial \bar{V}}{\partial \bar{Y}} = 0$$

(10)

The $\bar{X}$ and $\bar{Y}$components of an equation of motion are respectively given by

$$\rho\frac{\partial \bar{U}}{\partial \bar{t}} = div\,\bar{\tau} - \delta B_0{}^2\bar{U} - \frac{\mu(\bar{Y})}{k_0}\bar{U}$$

$$\rho\left(\frac{\partial \bar{U}}{\partial \bar{t}} + \bar{U}\frac{\partial \bar{U}}{\partial \bar{X}} + \bar{V}\frac{\partial \bar{U}}{\partial \bar{Y}}\right) = \frac{\partial \bar{\tau}_{XX}}{\partial \bar{X}} + \frac{\partial \bar{\tau}_{XY}}{\partial \bar{Y}} - \delta B_0{}^2\bar{U} - \frac{\mu(\bar{Y})}{k_0}\bar{U}$$

(11)

$$\rho\frac{\partial \bar{V}}{\partial \bar{t}} = div\,\bar{\tau} - \frac{\mu(\bar{Y})}{k_0}\bar{V}$$

$$\rho\left(\frac{\partial \bar{V}}{\partial \bar{t}} + \bar{U}\frac{\partial \bar{V}}{\partial \bar{X}} + \bar{V}\frac{\partial \bar{V}}{\partial \bar{Y}}\right) = \frac{\partial \bar{\tau}_{XY}}{\partial \bar{X}} + \frac{\partial \bar{\tau}_{YY}}{\partial \bar{Y}} - \frac{\mu(\bar{Y})}{k_0}\bar{V} \quad (12)$$

The energy equation becomes

$$\rho c_p\left[\frac{\partial \bar{T}}{\partial \bar{t}} + \bar{U}\frac{\partial \bar{T}}{\partial \bar{X}} + \bar{V}\frac{\partial \bar{T}}{\partial \bar{Y}}\right] = \kappa\left(\frac{\partial^2 \bar{T}}{\partial \bar{X}^2} + \frac{\partial^2 \bar{T}}{\partial \bar{Y}^2}\right) + \bar{S}.(grad\,\bar{U}) + \sigma B_0{}^2\,\bar{U}^2 + \frac{DK_T}{C_s}(\frac{\partial^2 C}{\partial \bar{X}^2} + \frac{\partial^2 C}{\partial \bar{Y}^2})$$

(13)

Equation of particles concentration

$$\frac{dC}{d\bar{t}} = D\nabla^2 C + \frac{DK_T}{T_m}(\frac{\partial^2 T}{\partial \bar{X}^2} + \frac{\partial^2 T}{\partial \bar{Y}^2}) \quad (14)$$

The boundary conditions can be written as:

$$\bar{U} = 0\,, \kappa\frac{\partial T}{\partial \bar{Y}} + \eta_1(T - T_0) = 0, C = C_1 \;\; at\;\; \bar{Y} = \bar{H}_1 \quad (15)$$

$$\bar{U} = 0\,, \kappa\frac{\partial T}{\partial \bar{Y}} + \eta_2(T_0 - T) = 0\,, C = C_0\; at\;\; \bar{Y} = \bar{H}_2 \quad (16)$$

In the fixed frame of reference $(\bar{X}, \bar{Y})$, the flow in the channel is unsteady.However, it can be treated as steady in a frame with coordinate system $(\bar{x}, \bar{y})$ moving with wave speed c (wave frame). The transformation equations relating the two frames are:

$$\bar{x} = \bar{X} - c\bar{t}\,, \bar{y} = \bar{Y}\,, \bar{u} = \bar{U}(\bar{X}, \bar{Y}, \bar{t}) - c\,, \bar{v} = \bar{V}(\bar{X}, \bar{Y}, \bar{t})$$

$$P(\bar{x}, \bar{y}) = P(\bar{X}, \bar{Y}, \bar{t})\,, T(\bar{x}, \bar{y}) = T(\bar{X}, \bar{Y}, \bar{t}), C(\bar{x}, \bar{y}) = C(\bar{X}, \bar{Y}, \bar{t}) \quad (17)$$

Introduce the following new dimensionless variables

$$x = \frac{2\pi\bar{x}}{\lambda},\; y = \frac{\bar{y}}{d_1},\; u = \frac{\bar{u}}{c},\; v = \frac{\bar{v}}{c}, p = \frac{2\pi d_1{}^2\bar{P}}{c\mu_0\lambda},\; h_1 = \frac{\bar{h}_1}{d_1},\; h_2 = \frac{\bar{h}_2}{d_2},\; t = \frac{2\pi c\bar{t}}{\lambda},\; \delta = \frac{2\pi d_1}{\lambda},\; Re = \frac{\rho c d_1}{\mu_0},\; \dot{\gamma} = \bar{\dot{\gamma}}\frac{\rho d^2}{\mu_0},\; s = \frac{d_1}{\mu_0 c}\bar{s},\; M^2 = \frac{\sigma B_0{}^2 d_1{}^2}{\mu_0},\; \mu(y) = \frac{\mu(\bar{y})}{\mu_0},\; Pr = \frac{\mu_0 c_p}{k}, Ec = \frac{c^2}{T_0 c_p}, Br = PrEc,\; \theta = \frac{T - T_0}{T_0},\; Bn = \frac{\tau_y d_1}{\mu_0 c}, \Phi = \frac{C - C_0}{C_1 - C_0}, Sc = \frac{v}{D}, Sr = \frac{DK_T T_0}{vT_m(C_1 - C_0)}, D_u = \frac{DK_T T_0(C_1 - C_0)}{\mu_0 c_p\, C_p\, T_0}$$

(18)

Where p is the pressure, $(h_1,\; h_2)$ is the channel walls, δ is the wave number, Re is the Reynolds number, M is the Hartman number, Pr is the Prandtl number, Ec is the Eckert number, Br is the Brinkman number, θ is the temperature, Bn is the Bingham number, Sc is the Schmidt number, Sr is the Soret number, and D_u is the Dufour number. Substituting Eq.(18) with equations (10) - (14) . And if $\psi(x, y, t)$ is the stream function then the velocity components in terms of stream function are:

$$u = \frac{\partial \psi}{\partial y}\,, v = -\delta\frac{\partial \psi}{\partial x} \quad (19)$$

In view of the lubrication approach method and stream function Eq.(19) with Eqs.(10)-(14) we get:

$$\frac{\partial P}{\partial x} = \frac{\partial S_{xy}}{\partial y} - (M^2 + \frac{\mu(y)}{k})(\frac{\partial \psi}{\partial y} + 1) \quad (20)$$

$$\frac{\partial P}{\partial y} = 0$$

(21)

$$\frac{\partial^2 \theta}{\partial y^2} + Br\,\left(\frac{\partial}{\partial y}(\frac{\partial \psi}{\partial y})\right)s_{xy} + BrM^2(\frac{\partial \psi}{\partial y} + 1)^2 + Du\,Pr\frac{\partial^2 \Phi}{\partial y^2} = 0$$

(22)

$$\frac{1}{Sc}\frac{\partial^2 \Phi}{\partial y^2} + Sr\frac{\partial^2 \theta}{\partial y^2} = 0$$

(23)

The stress component of Bingham plastic fluid which we worked on in this paper, which reads as follows:

$$s_{xy} = \mu(y)\left(\frac{\partial^2 \psi}{\partial y^2}\right) + B_n$$

(24)

Where B_n is called Bingham number. And $\mu(y) = 1 - \alpha y$.

4. Method of solution:

From the equations resulting of the motion equation, it becomes apparent that P is independent of y. and it is not linear. It seems to be impossible to obtain a general solution in closed form for an orbitary power series expansion in terms of small parameter α (Regular perturbation technique) thus the stream function, temperature distribution and concentration distribution will be written as:

$\psi = \psi_0 + \alpha\psi_1 + \cdots$
$\theta = \theta_0 + \alpha\theta_1 + \cdots$
$\Phi = \Phi_0 + \alpha\Phi_1 + \cdots$ (25)

Putting the above quantities (25) into the equations (20), (22) and (23), then collecting the terms of like power of α, we get the following zeroth and first order systems.

4.1 Zeroth order systems α^0

The coefficients of α^0 arrive at

$$\frac{\partial^4\psi_0}{\partial y^4} - (M^2 + \frac{1}{k})\frac{\partial^2\psi_0}{\partial y^2} = 0$$
(26)

$$\frac{\partial^2\theta_0}{\partial y^2} + Br\,(\frac{\partial^2\theta_0}{\partial y^2})^2 + BnBr\frac{\partial^2\psi_0}{\partial y^2} + BrM^2(\frac{\partial\psi_0}{\partial y} + 1)^2 + Du\,Pr\frac{\partial^2\Phi_0}{\partial y^2} = 0 \quad (27)$$

$$\frac{1}{Sc}\frac{\partial^2\Phi_0}{\partial y^2} + Sr\frac{\partial^2\theta_0}{\partial y^2} = 0 \quad (28)$$

Along with the corresponding boundary conditions

$$\psi_0 = \frac{F_0}{2}, \frac{\partial\psi_0}{\partial y} = -1, \frac{\partial\theta}{\partial y} + v_1\theta = 0, \Phi = 1 \quad at\ (y = h_1)$$
$$\psi_0 = -\frac{F_0}{2}, \frac{\partial\psi_0}{\partial y} = -1, \frac{\partial\theta}{\partial y} - v_2\theta = 0, \Phi = 0 \quad at\ (y = \mathrm{h}_2)$$
(29)

In which F is the flow rate in a wave frame

4.2 First order systems: α^1

The coefficients of α^1 arrive

$$\left(\frac{\partial^4\psi_1}{\partial y^4} - y\frac{\partial^4\psi_0}{\partial y^4} - 2\frac{\partial^3\psi_0}{\partial y^3}\right) - \left(M^2 + \frac{1}{k}\right)\frac{\partial^2\psi_1}{\partial y^2} + \frac{y}{k}\frac{\partial^2\psi_0}{\partial y^2} + \frac{1}{k}(\frac{\partial\psi_0}{\partial y} + 1) = 0 \quad (30)$$

$$\frac{\partial^2\theta_1}{\partial y^2} + 2Br\,\frac{\partial^2\psi_0}{\partial y^2}\frac{\partial^2\psi_1}{\partial y^2} - yBr\left(\frac{\partial^2\psi_0}{\partial y^2}\right)^2 + BnBr\frac{\partial^2\psi_1}{\partial y^2} + 2BrM^2\left(\frac{\partial\psi_0}{\partial y} + 1\right)^2\frac{\partial\psi_1}{\partial y} + Du\,Pr\frac{\partial^2\Phi_1}{\partial y^2} = 0 \quad (31)$$

$$\frac{1}{Sc}\frac{\partial^2\Phi_1}{\partial y^2} + Sr\frac{\partial^2\theta_1}{\partial y^2} = 0 \quad (32)$$

Along with the corresponding boundary conditions

$$\psi_1 = \frac{F_1}{2}, \frac{\partial\psi_1}{\partial y} = 0, \frac{\partial\theta}{\partial y} + v_1\theta = 0, \Phi = 1 \quad at\ (y = h_1)$$
$$\psi_1 = -\frac{F_1}{2}, \frac{\partial\psi_1}{\partial y} = 0, \frac{\partial\theta}{\partial y} - v_2\theta = 0, \Phi = 0 \quad at\ (y = \mathrm{h}_2)$$
(33)

In which F is the flow rate in a wave frame.

The solution of the equations (26-28) together with the boundary condition and equations (30-32) together with the boundary condition are obtained by using a mathematical program

5. RESULT AND DISCUSSION:

In this section we study and discuss the variation of various parameters on the behavior of pressure gradient $\frac{dP}{dx}$, pressure rise per wave length ΔP_λ, velocity, temperature, concentration and stream function.

5.1 Temperature distribution:

The graphical results for the heat transfer phenomenon are discussed in figs. (2)- (14).Fig. (2) shows the influence of viscosity parameter α on temperature profile θ. It is observed that due to convective conditions temperature at the boundaries is minimum while it is maximum at the center of the channel. Fig (3) shows that increasing Hartman number M increases the temperature profile from the begging to the end of the channel. Fig. (4) depicts that the temperature profile is an increasing function in relation to the increase of F_0.Fig. (5) shows that the temperature profile is an increasing function to in relation the increase of the first Biot number and fig. (6) shows that the temperature profile is decreasing for large values for the second Biot number. Fig. (7) indicates that the temperature profile is an increasing function of B_r. It is witnessed that the viscous dissipation will be greater according to the thermal boundary layer thickness. It is evident that the temperature is zero when f $B_r = 0$. Fig. (8) indicates that the temperature profile increase by the increasing of the Prandt number since the temperature variations in the flow are due to viscous dissipation thus the Prandt number being directly related to viscosity support of the penetration depth of the temperature. Fig. (9) portrays the increasing of the Bingham number B_n to the maximum of the temperature profile from the beginning to the center; and to the minimum of the temperature profile at the end of the channel. Fig. (10) and (11) show that the temperature profile is an increasing function for the increasing of the wall damping coefficient r_1, r_2. Figs. (12) and (13) indicate the influence of the Dufore number Du and the Soret number Sr effect on the temperature profile. The temperature profile is an increasing function according to the increasing of the Dufore number and the Soret number. The Soret effect become clear when there is sheer temperature gradient thus the thermal boundary layer becomes thicker through the increasing of the Soret number. Fig. (14) shows that the temperature profile increase through the increasing of the Schmidt number Sc. Since Sc is directly proportionate to viscosity.

5.2 Concentration distribution:

Variations to different parameters on the concentration profile are portrayed in Figs. (15)- (27). Fig. (15) indicates that an increase of the viscosity parameter α decreases the concentration profile. In fact the concentration for constant viscosity $(\alpha = 0)$ is greater than the variable viscosity$(\alpha \neq 0)$. Fig (16) shows that increasing the Hartman number M decreases the concentration profile. Fig. (17) Shows that the concentration profile decrease by the increase of F_0. Figs. (18) and (19) show that the concentration profile is an increasing function according to the increase of the first and the second Biot number. Figs. (20) and (21) show that an increasing of the Brinkman number and the Prandt number respectively decrease the concentration profile but the Prandt number is more effective on the concentration profile than Brinkman number. Fig. (22) portrays the increasing of the Bingham number B_n to a minimum of the concentration profile from the begining to the center and to a maximum of the concentration profile at the end of the channel. Figs. (23) and (24) show that the concentration profile is a decreasing function for the increasing of wall damping coefficients r_1, r_2. Figs. (25) and (26) show the influence of the Dufore number Du and the Soret number Sr effect on the concentration profile respectively. The concentration profile is a decreasing function for the increasing of the Dufore number and the Soret number. The Dufore number Du effect is dominant compared to the Soret number Sr on the concentration profile. Fig. (27) shows that the concentration profile is a decreasing function if the Schmidt number Sc increases.

5.3 Behavior of pressure gradient

The main focus of this section is to describe the behavior of pressure gradient $\frac{dP}{dx}$ with a variation in parameters. Plots of the pressure gradient $\frac{dP}{dx}$ versus axial difference x for various parameters are shown in figs. (28-34). Fig. (28) shows the effect of the phase difference on the pressure gradient $\frac{dP}{dx}$ where $\frac{dP}{dx}$ increases in the lower part of the channel by the increase of a phase difference and inverse behavior on the upper part of the channel. Fig.(29) depicts that the viscosity effect on the pressure gradient $\frac{dP}{dx}$ is such that an increase in the viscosity parameter reduces the effect of pressure gradient $\frac{dP}{dx}$ on the flow because in the lower and upper parts of the channel, pressure gradient $\frac{dP}{dx}$ decreases by increasing the viscosity, and in the central of the channel it is inversely. Thus we conclude that the pressure gradient $\frac{dP}{dx}$ in viscous fluids is greater than in Bingham plastic fluids. Fig.(30) reveals that pressure gradient $\frac{dP}{dx}$ is inversely proportional to the Hartman number M. Fig.(31) shows that an increase in the parameter k leads to an increase in pressure gradient $\frac{dP}{dx}$. Fig.(32) shows that pressure gradient $\frac{dP}{dx}$ is inversely proportional to F_0. Figs (33) and (34) show the effect of changing the wall damping coefficient on pressure gradient $\frac{dP}{dx}$ where Fig. (33) in the lower and upper parts of the channel decrease by increasing the first wall damping coefficient. Fig.(34) shows that pressure gradient $\frac{dP}{dx}$ is inversely proportional to the second wall damping coefficient.

5.4 Velocity distribution:

The flowing figures show the behavior of parameters involved in the axial velocity u. The variation of velocity for different values of $\phi, \alpha, M, F0, k, r1,$ r2 are illustrated in figs. (35-41). It is noticed that the pattern of the velocity profiles are parabolic and velocity increases mostly in the central line of the channel. Fig.(35) shows the effect of changing the phase difference ϕ on the velocity axial u, the velocity increases from the lower part of the channel and marge from the central line of the channel to the upper part of the channel. Fig.(36) shows the effect of variations in viscosity α on the velocity axial u. At the lower part of the channel, the viscosity increases but the velocity decreases. Throughout the rest of the channel the velocity increases as the viscosity increase. Fig.(37) shows the effect of the Hartman number M. We notice at the lower part of the channel that the velocity axial u increase as the Hartman number increases, at the central line of the channel the velocity axial u decreases as the Hartman number increase, and at the upper part of the channel the velocity axial u increases as the Hartman number increases. Fig.(38) shows the effects of $F0$ on the velocity axial u, where at the lower part of the channel the velocity axial u decreases as $F0$ increase, at the central line of the channel the velocity axial u increases as $F0$ increases, and at the upper part of the channel the velocity axial u decreases as $F0$ increase. Fig. (39) shows the effects of k on the velocity axial u ,It can easily be noticed that the velocity exhibits oscillating behavior if we change the parameter k. Fig.(40) shows the effects of the 1st wall damping parameter $r1$ on the velocity axial u where we notice at the lower part of the channel that the velocity axial u increases as $r1$ increases, at the central line of the channel the velocity axial u decreases as $r1$ increases, and at the upper part of the channel the velocity axial u increases as $r1$ increases. Fig.(41) shows the effects of the 2nd wall damping parameter $r2$ on the velocity axial u where we notice at the lower part of the channel that the velocity axial u increases as $r2$ increases, and marge from the central line of the channel to the rest of the channel.

5.5 Trapping phenomenon:

Trapping is an interesting phenomenon in peristalsis. The shape of streamlines is similar to the wave shape traveling across the channel walls. A phenomenon in which these streamlines split and enclose a bolus which moves as a whole under certain conditions. Streamlines behavior for different sundry parameters is depicted in the following figures. The streamlines for different values of phase difference are shown in fig.(42). It is observed that the size of bolus decreases as the value of ϕ increases. Fig.(43) shows the effect of the increase of the Hartman number on the streamlines. It is observed that trapped bolus decreases with the increasing of M. Fig.(44) is plotted to see the effects of viscosity α on the streamlines.

It is observed that trapped bolus increases with the increasing of viscosity. Fig.(45) indicates the effect of increasing F0 on streamlines, where the size of the trapped bolus are going to increase. Fig.(46) indicates the effect of thermal conductivity k. The increasing of k shows no change on the size of trapped bolus, where it remains the same. The effect of the first wall damping parameter r_1 can be seen in fig.(47). It is observed that when we increase r_1 the size of the trapped bolus increases. The effect of the second wall damping parameter r_2 can be seen in fig.(48). It is observed that when we increase r_2 the size of the trapped bolus increase.

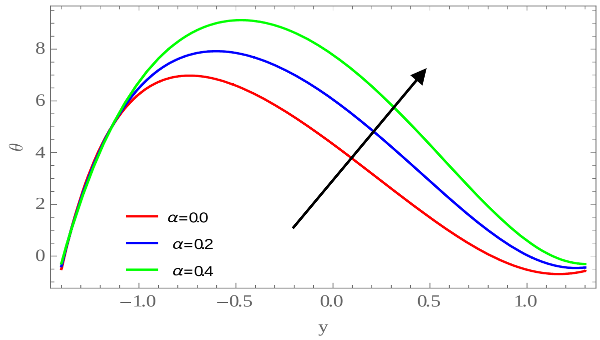

Fig. (2): effect of α on θ [$\phi = \frac{\pi}{6}, M = 0.5, k = 0.2, r_1 = 0.5, r_2 = 0.3, F0 = 0.1, Du = 0.5, Sr = 0.8, Sc = 0.5, Bi1 = 10, Bi2 = 10, Bn = 4, Pr = 2, Br = 2$]

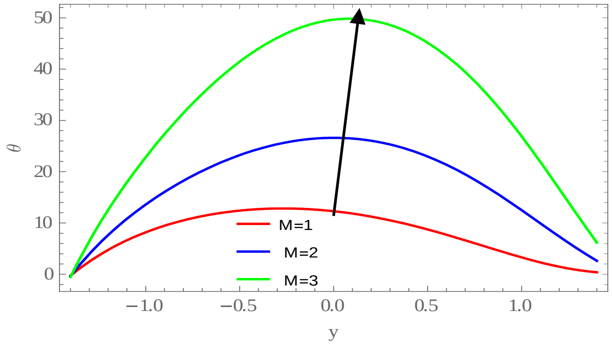

Fig. (3): effect of M on θ [$\alpha = 0.5, \phi = \frac{\pi}{6}, k = 0.2, r_1 = 0.5, r_2 = 0.3, F0 = 0.1, Du = 0.5, Sr = 0.8, Sc = 0.5, Bi1 = 10, Bi2 = 10, Bn = 4, Pr = 2, Br = 2$]

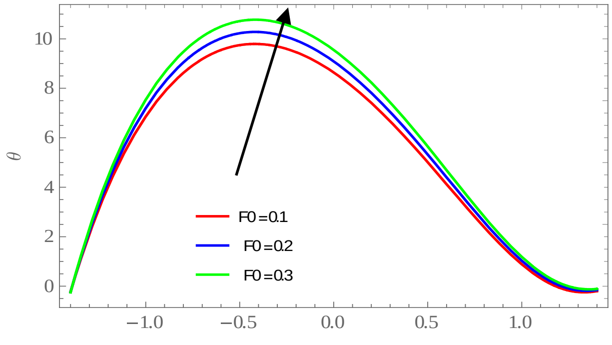

Fig. (4): effect of $F0$ on θ [$\alpha = 0.5, \phi = \frac{\pi}{6}, M = 0.5, k = 0.2, r_1 = 0.5, r_2 = 0.3, Du = 0.5, Sr = 0.8, Sc = 0.5, Bi1 = 10, Bi2 = 10, Bn = 4, Pr = 2, Br = 2$]

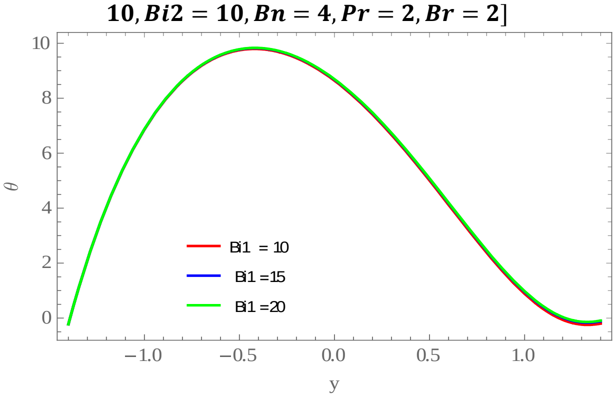

Fig. (5): effect of $Bi1$ on θ [$\alpha = 0.5, \phi = \frac{\pi}{6}, M = 0.5, k = 0.2, r_1 = 0.5, r_2 = 0.3, F0 = 0.1, Du = 0.5, Sr = 0.8, Sc = 0.5, Bi2 = 10, Bn = 4, Pr = 2, Br = 2$

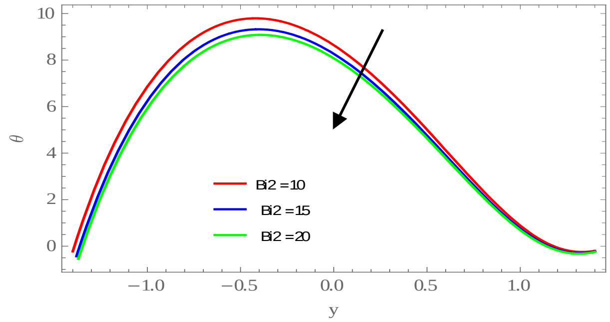

Fig. (6): effect of $Bi2$ on θ [$\alpha = 0.5, \phi = \frac{\pi}{6}, M = 0.5, k = 0.2, r_1 = 0.5, r_2 = 0.3, F0 = 0.1, Du = 0.5, Sr = 0.8, Sc = 0.5, Bi1 = 10, Bn = 4, Pr = 2, Br = 2$]

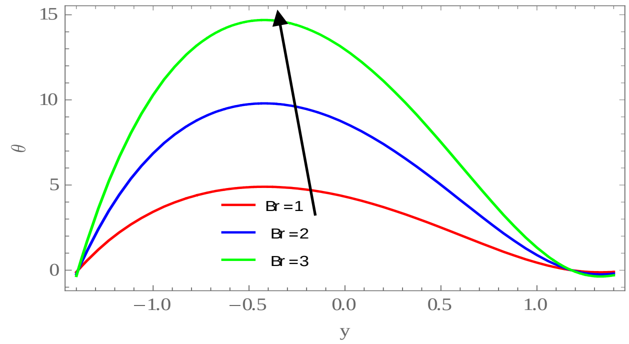

Fig. (7): effect of Br on θ [$\alpha = 0.5, \phi = \frac{\pi}{6}, M = 0.5, k = 0.2, r_1 = 0.5, r_2 = 0.3, F0 = 0.1, Du = 0.5, Sr = 0.8, Sc = 0.5, Bi1 = 10, Bi2 = 10, Bn = 4, Pr = 2$]

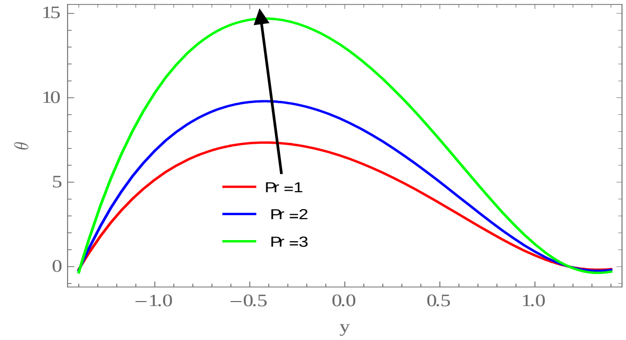

Fig. (8): effect of Pr on θ [$\alpha = 0.5, \phi = \frac{\pi}{6}, M = 0.5, k = 0.2, r_1 = 0.5, r_2 = 0.3, F0 = 0.1, Du = 0.5, Sr = 0.8, Sc = 0.5, Bi1 = 10, Bi2 = 10, Bn = 4, Br = 2$]

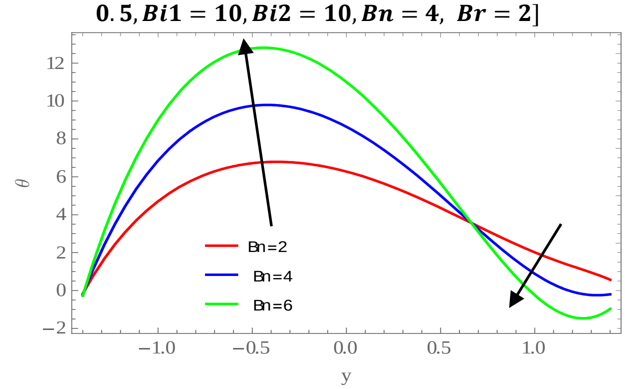

Fig. (9): effect of Bn on θ [$\alpha = 0.5, \phi = \frac{\pi}{6}, M = 0.5, k = 0.2, r_1 = 0.5, r_2 = 0.3, F0 = 0.1, Du = 0.5, Sr = 0.8, Sc = 0.5, Bi1 = 10, Bi2 = 10, Pr = 2, Br = 2$]

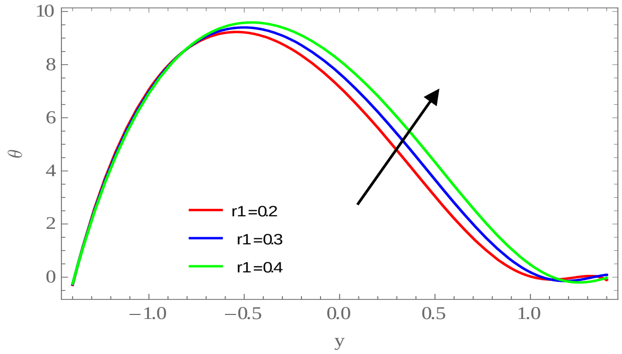

Fig. (10): effect of $r1$ **on** θ $[\alpha = 0.5, \phi = \frac{\pi}{6}, M = 0.5, k = 0.2, r_2 = 0.3, F0 = 0.1, Du = 0.5, Sr = 0.8, Sc = 0.5, Bi1 = 10, Bi2 = 10, Bn = 4, Pr = 2, Br = 2]$

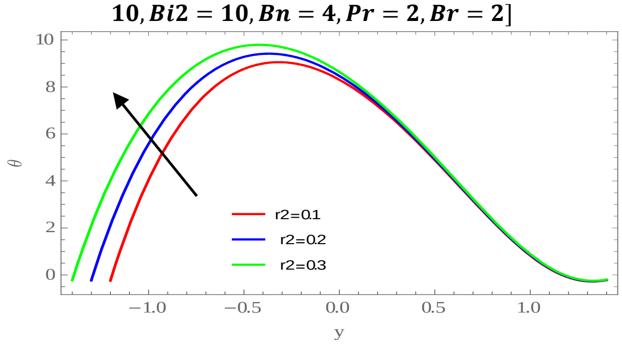

Fig. (11): effect of $r2$ **on** θ $[\alpha = 0.5, \phi = \frac{\pi}{6}, M = 0.5, k = 0.2, r_1 = 0.5, F0 = 0.1, Du = 0.5, Sr = 0.8, Sc = 0.5, Bi1 = 10, Bi2 = 10, Bn = 4, Pr = 2, Br = 2]$

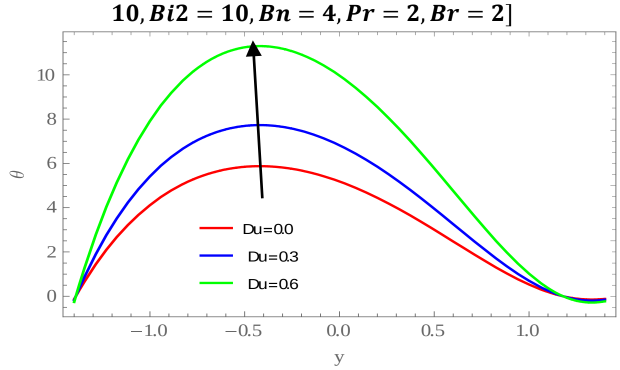

Fig. (12): effect of Du **on** θ $[\alpha = 0.5, \phi = \frac{\pi}{6}, M = 0.5, k = 0.2, r_1 = 0.5, r_2 = 0.3, F0 = 0.1, Sr = 0.8, Sc = 0.5, Bi1 = 10, Bi2 = 10, Bn = 4, Pr = 2, Br = 2]$

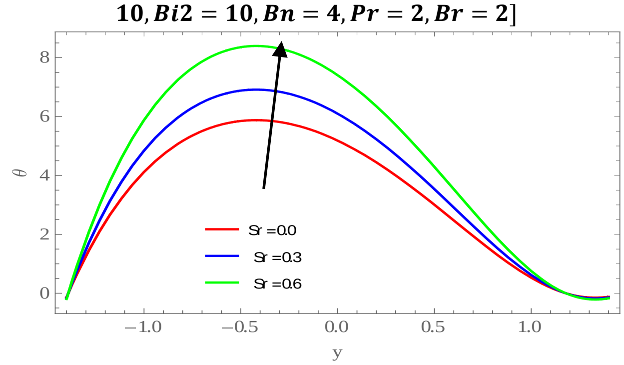

Fig. (13): effect of Sr **on** θ $[\alpha = 0.5, \phi = \frac{\pi}{6}, M = 0.5, k = 0.2, r_1 = 0.5, r_2 = 0.3, F0 = 0.1, Du = 0.5, S, Sc = 0.5, Bi1 = 10, Bi2 = 10, Bn = 4, Pr = 2, Br = 2]$

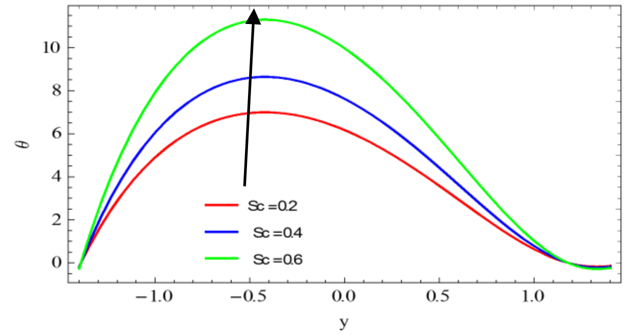

Fig. (14): effect of Sc **on** θ $[\alpha = 0.5, \phi = \frac{\pi}{6}, M = 0.5, k = 0.2, r_1 = 0.5, r_2 = 0.3, F0 = 0.1, Du = 0.5, Sr = 0.8, Bi1 = 10, Bi2 = 10, Bn = 4, Pr = 2, Br = 2]$

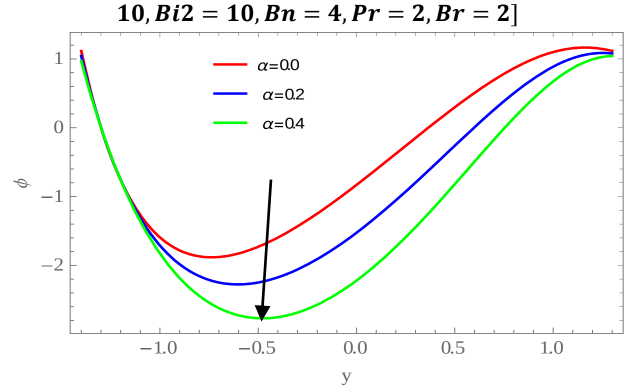

Fig. (15): effect of α **on** Φ $[\phi = \frac{\pi}{6}, M = 0.5, k = 0.2, r_1 = 0.5, r_2 = 0.3, F0 = 0.1, Du = 0.5, Sr = 0.8, Sc = 0.5, Bi1 = 10, Bi2 = 10, Bn = 4, Pr = 2, Br = 2]$

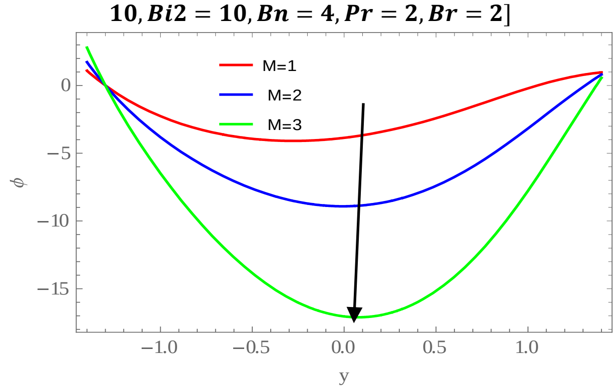

Fig. (16): effect of M **on** Φ $[\alpha = 0.5, \phi = \frac{\pi}{6}, k = 0.2, r_1 = 0.5, r_2 = 0.3, F0 = 0.1, Du = 0.5, Sr = 0.8, Sc = 0.5, Bi1 = 10, Bi2 = 10, Bn = 4, Pr = 2, Br = 2]$

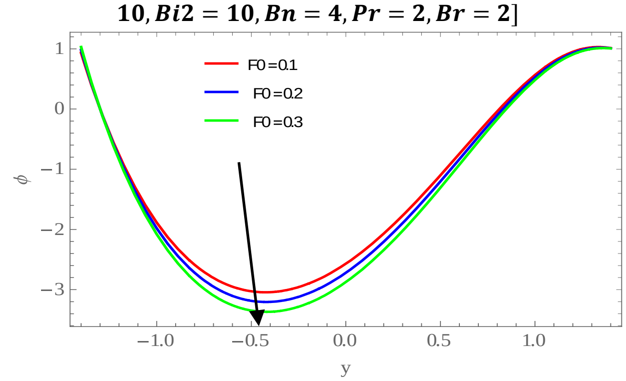

Fig. (17): effect of $F0$ **on** Φ $[\alpha = 0.5, \phi = \frac{\pi}{6}, M = 0.5, k = 0.2, r_1 = 0.5, r_2 = 0.3, Du = 0.5, Sr = 0.8, Sc = 0.5, Bi1 = 10, Bi2 = 10, Bn = 4, Pr = 2, Br = 2]$

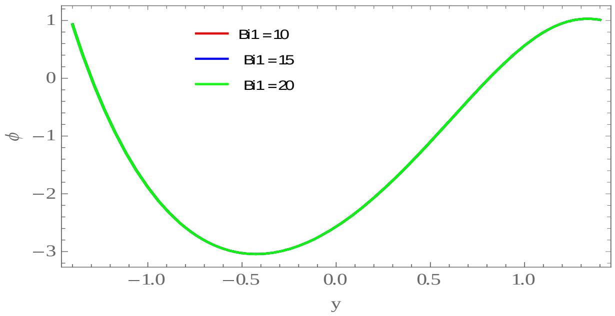

Fig. (18): effect of $\boldsymbol{Bi1}$ **on** $\boldsymbol{\Phi}$ $\boldsymbol{[\alpha = 0.5, \phi = \frac{\pi}{6}, M = 0.5, k = 0.2, r_1 = 0.5, r_2 = 0.3, F0 = 0.1, Du = 0.5, Sr = 0.8, Sc = 0.5, Bi2 = 10, Bn = 4, Pr = 2, Br = 2]}$

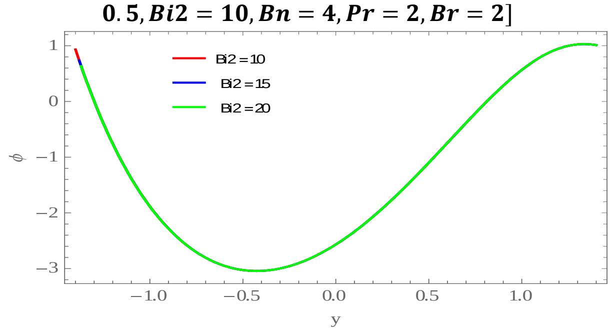

Fig. (19): effect of $\boldsymbol{Bi2}$ **on** $\boldsymbol{\Phi}$ $\boldsymbol{[\alpha = 0.5, \phi = \frac{\pi}{6}, M = 0.5, k = 0.2, r_1 = 0.5, r_2 = 0.3, F0 = 0.1, Du = 0.5, Sr = 0.8, Sc = 0.5, Bi1 = 10, Bn = 4, Pr = 2, Br = 2]}$

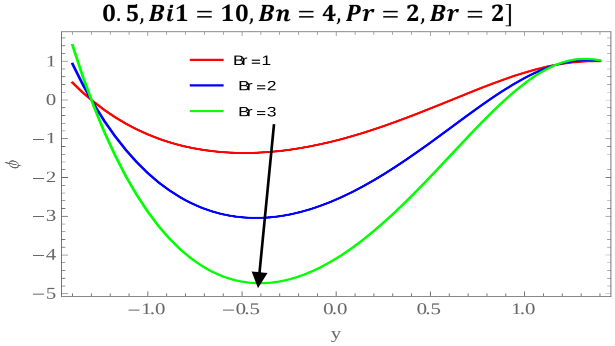

Fig. (20): effect of $\boldsymbol{Br}$ **on** $\boldsymbol{\Phi}$ $\boldsymbol{[\alpha = 0.5, \phi = \frac{\pi}{6}, M = 0.5, k = 0.2, r_1 = 0.5, r_2 = 0.3, F0 = 0.1, Du = 0.5, Sr = 0.8, Sc = 0.5, Bi1 = 10, Bi2 = 10, Bn = 4, Pr = 2]}$

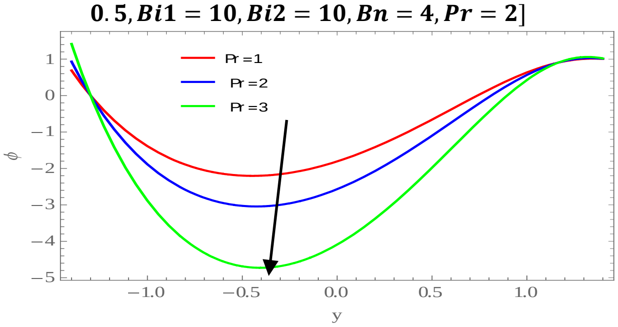

Fig. (21): effect of $\boldsymbol{Pr}$ **on** $\boldsymbol{\Phi}$ $\boldsymbol{[\alpha = 0.5, \phi = \frac{\pi}{6}, M = 0.5, k = 0.2, r_1 = 0.5, r_2 = 0.3, F0 = 0.1, Du = 0.5, Sr = 0.8, Sc = 0.5, Bi1 = 10, Bi2 = 10, Bn = 4, Br = 2]}$

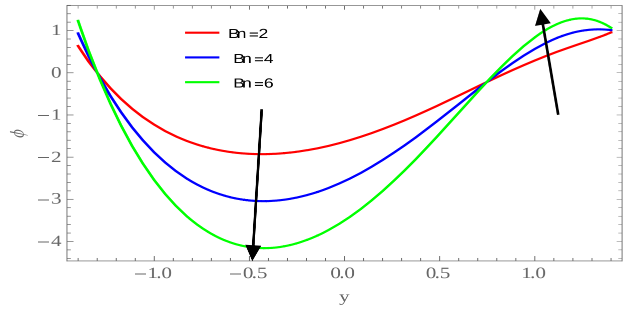

Fig. (22): effect of $\boldsymbol{Bn}$ **on** $\boldsymbol{\Phi}$ $\boldsymbol{[\alpha = 0.5, \phi = \frac{\pi}{6}, M = 0.5, k = 0.2, r_1 = 0.5, r_2 = 0.3, F0 = 0.1, Du = 0.5, Sr = 0.8, Sc = 0.5, Bi1 = 10, Bi2 = 10, Pr = 2, Br = 2]}$

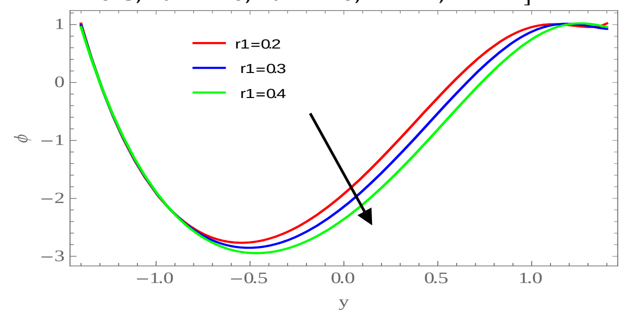

Fig. (23): effect of $\boldsymbol{r1}$ **on** $\boldsymbol{\Phi}$ $\boldsymbol{[\alpha = 0.5, \phi = \frac{\pi}{6}, M = 0.5, k = 0.2, r_2 = 0.3, F0 = 0.1, Du = 0.5, Sr = 0.8, Sc = 0.5, Bi1 = 10, Bi2 = 10, Bn = 4, Pr = 2, Br = 2]}$

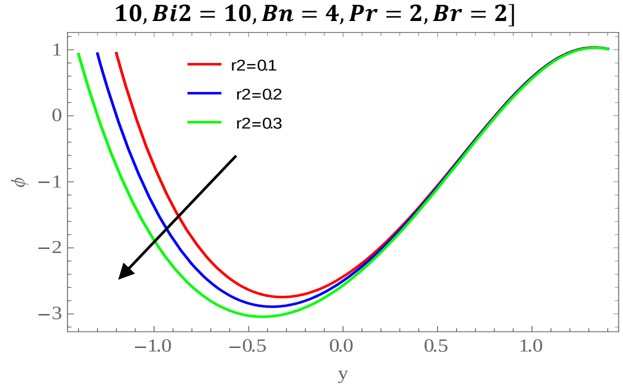

Fig. (24): effect of $\boldsymbol{r2}$ **on** $\boldsymbol{\Phi}$ $\boldsymbol{[\alpha = 0.5, \phi = \frac{\pi}{6}, M = 0.5, k = 0.2, r_1 = 0.5, F0 = 0.1, Du = 0.5, Sr = 0.8, Sc = 0.5, Bi1 = 10, Bi2 = 10, Bn = 4, Pr = 2, Br = 2]}$

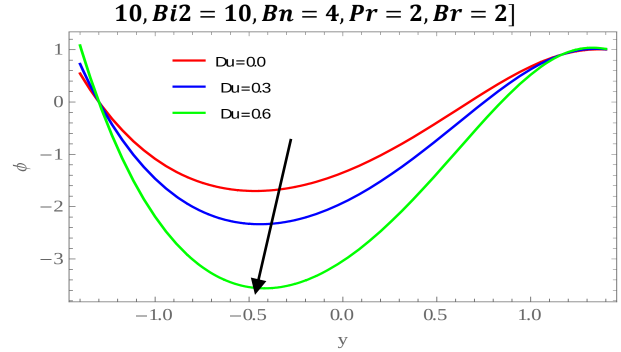

Fig. (25): effect of $\boldsymbol{Du}$ **on** $\boldsymbol{\Phi}$ $\boldsymbol{[\alpha = 0.5, \phi = \frac{\pi}{6}, M = 0.5, k = 0.2, r_1 = 0.5, r_2 = 0.3, F0 = 0.1, Sr = 0.8, Sc = 0.5, Bi1 = 10, Bi2 = 10, Bn = 4, Pr = 2, Br = 2]}$

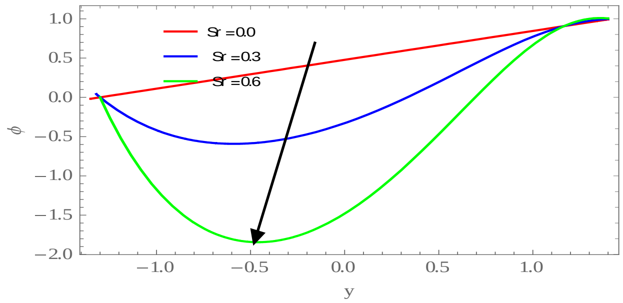

Fig. (26): effect of Sr on Φ [$\alpha = 0.5, \phi = \frac{\pi}{6}, M = 0.5, k = 0.2, r_1 = 0.5, r_2 = 0.3, F0 = 0.1, Du = 0.5, Sc = 0.5, Bi1 = 10, Bi2 = 10, Bn = 4, Pr = 2, Br = 2$]

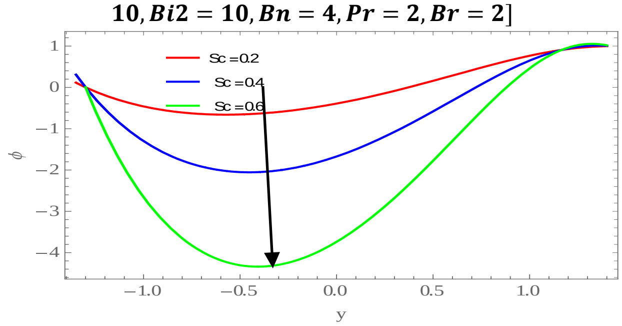

Fig. (27): effect of Sc on Φ [$\alpha = 0.5, \phi = \frac{\pi}{6}, M = 0.5, k = 0.2, r_1 = 0.5, r_2 = 0.3, F0 = 0.1, Du = 0.5, Sr = 0.8, Bi1 = 10, Bi2 = 10, Bn = 4, Pr = 2, Br = 2$]

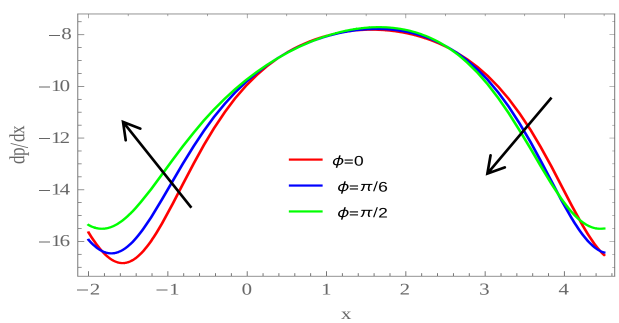

Fig. (28): Pressure gradient $\frac{dP}{dx}$ versus axial distance x when $\alpha = 0.5, M = 0.5, k = 0.2, r1 = 0.5, r2 = 0.3, F0 = 0.1, F1 = 0$

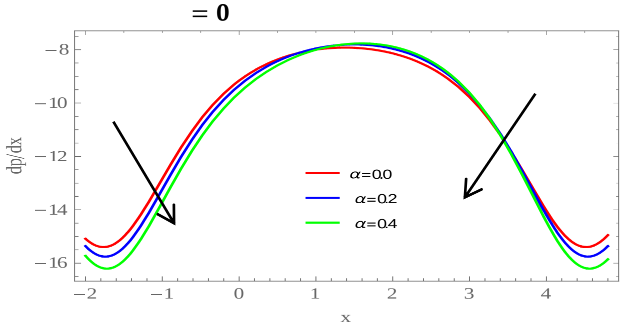

Fig. (29): Pressure gradient $\frac{dP}{dx}$ versus axial distance x when $\phi = \pi/6,, M = 0.5, k = 0.2, r1 = 0.5, r2 = 0.3, F0 = 0.1, F1 = 0$

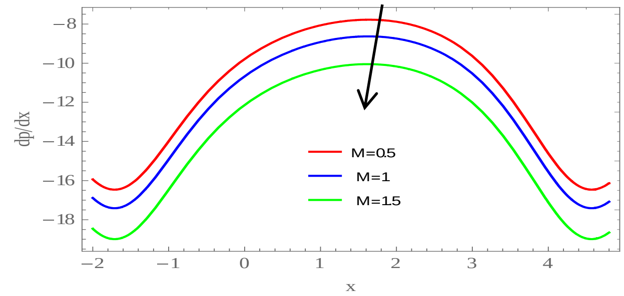

Fig. (30): Pressure gradient $\frac{dP}{dx}$ versus axial distance x when $\phi = \pi/6, \alpha = 0.5, k = 0.2, r1 = 0.5, r2 = 0.3, F0 = 0.1, F1 = 0$

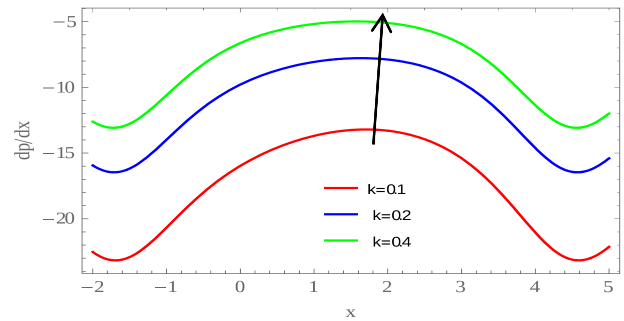

Fig. (31): Pressure gradient $\frac{dP}{dx}$ versus axial distance x when $\phi = \pi/6, \alpha = 0.5, M = 0.5, r1 = 0.5, r2 = 0.3, F0 = 0.1, F1 = 0$

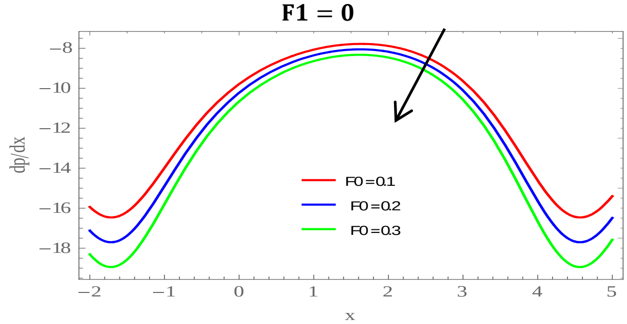

Fig. (32): Pressure gradient $\frac{dP}{dx}$ versus axial distance x when $\phi = \pi/6, \alpha = 0.5, M = 0.5, k = 0.2, r1 = 0.5, r2 = 0.3, F1 = 0.$

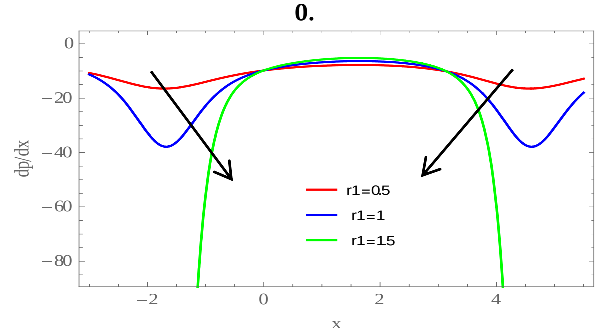

Fig. (33): Pressure gradient $\frac{dP}{dx}$ versus axial distance x when $\phi = \pi/6, \alpha = 0.5, M = 0.5, k = 0.2, r2 = 0.3, F0 = 0.1, F1 = 0$

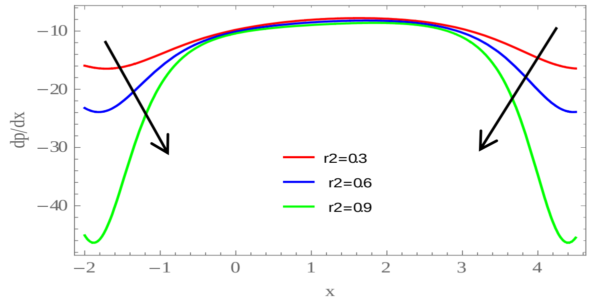

Fig. (34): Pressure gradient $\frac{dP}{dx}$ versus axial distance x when $\phi = \pi/6, \alpha = 0.5, M = 0.5, k = 0.2, \mathrm{r1} = 0.5, \mathrm{F0} = 0.1, \mathrm{F1} = 0$

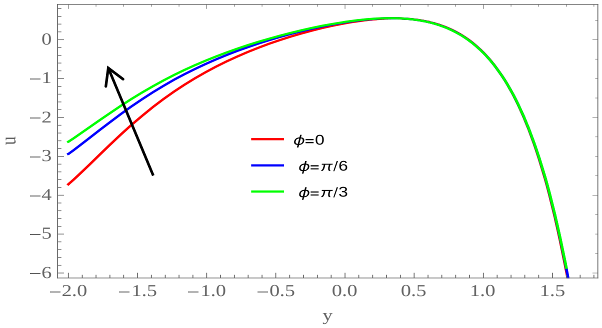

Fig. (35): effects of ϕ on u when $\alpha = 0.5, M = 0.5, k = 0.2, \mathrm{r1} = 0.5, \mathrm{r2} = 0.3, \mathrm{F0} = 0.1, \mathrm{F1} = 0$

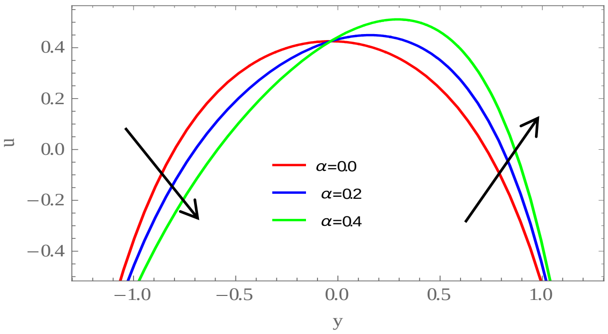

Fig. (36): effects of α on u when $\phi = \pi/6, M = 0.5, k = 0.2, \mathrm{r1} = 0.5, \mathrm{r2} = 0.3, \mathrm{F0} = 0.1, \mathrm{F1} = 0,$

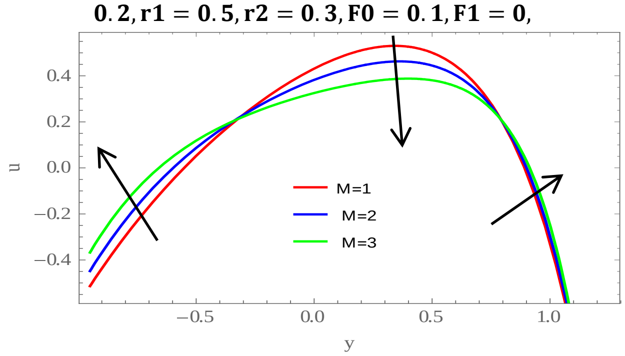

Fig.(37): effects of M on u when $\phi = \pi/6, \alpha = 0.5, k = 0.2, \mathrm{r1} = 0.5, \mathrm{r2} = 0.3, \mathrm{F0} = 0.1, \mathrm{F1} = 0,$

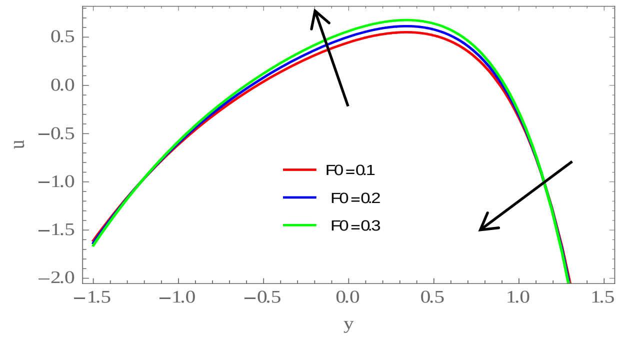

Fig. (38): effects of $F0$ on u when $\phi = \pi/6, \alpha = 0.5, M = 0.5, k = 0.2, \mathrm{r1} = 0.5, \mathrm{r2} = 0.3, \mathrm{F1} = 0$

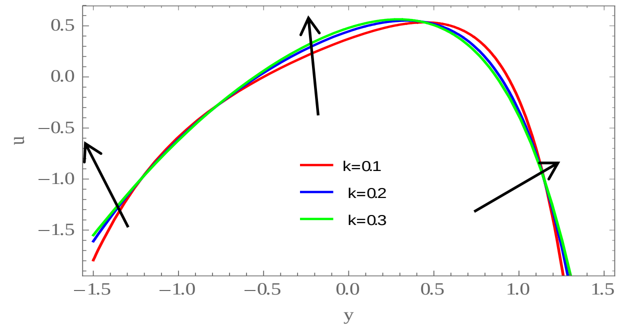

Fig. (39): effects of k on u when $\phi = \pi/6, \alpha = 0.5, M = 0.5, \mathrm{r1} = 0.5, \mathrm{r2} = 0.3, \mathrm{F0} = 0.1, \mathrm{F1} = 0$

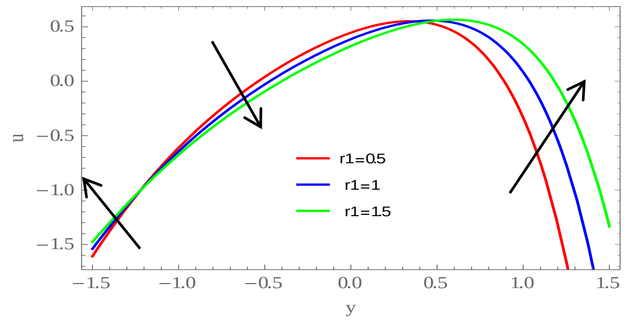

Fig. (40): effects of $r1$ on u when $\phi = \pi/6, \alpha = 0.5, M = 0.5, \mathrm{k} = 0.2, \mathrm{r2} = 0.3, \mathrm{F0} = 0.1, \mathrm{F1} = 0$

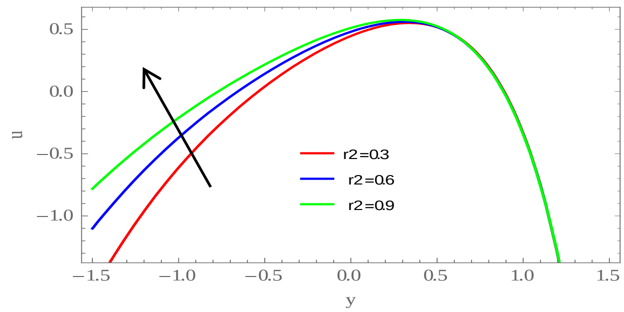

Fig. (41): effects of $r2$ on u when $\phi = \pi/6, \alpha = 0.5, M = 0.5, k = 0.2, \mathrm{r1} = 0.5, \mathrm{F0} = 0.1, \mathrm{F1} = 0$

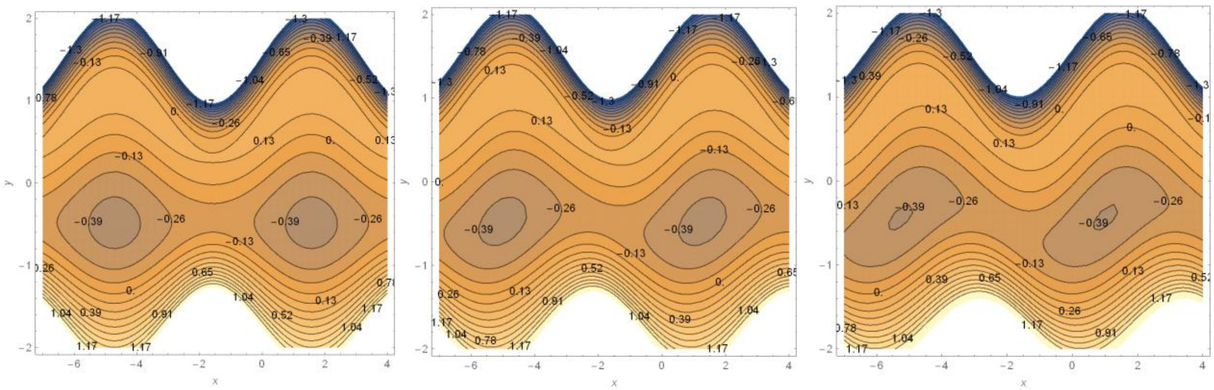

Fig.(42): effect of phase difference

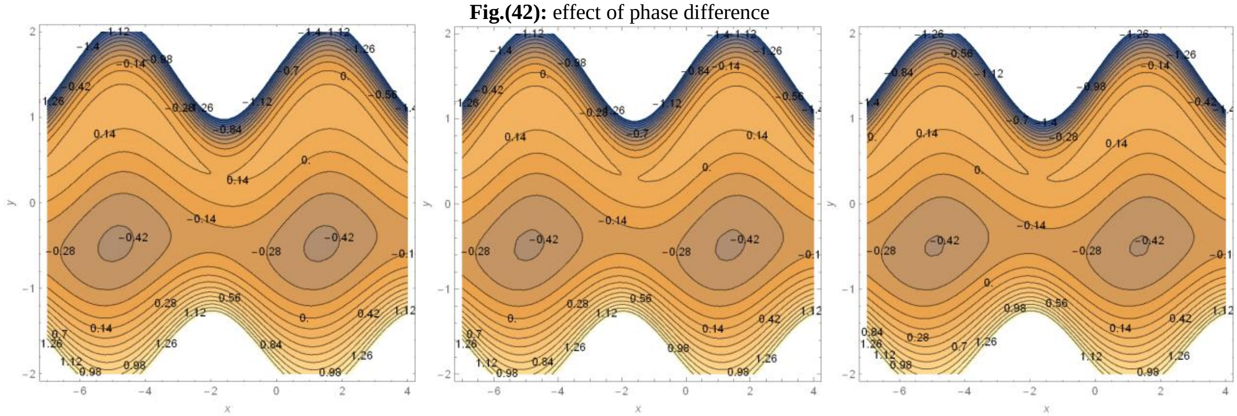

Fig.(43): effect of Hartman number

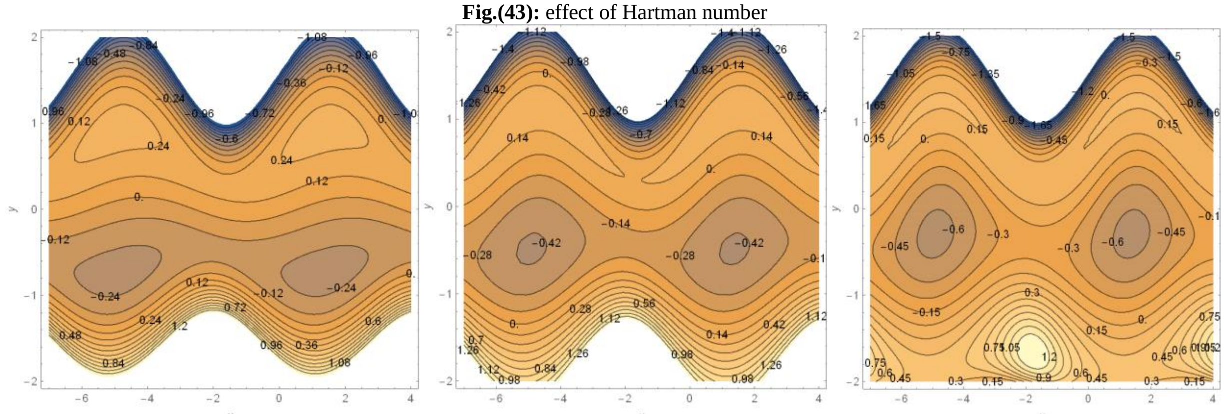

Fig.(44): effect of viscosity ($\alpha = 0.0, \alpha = 0.5, \alpha = 1$)

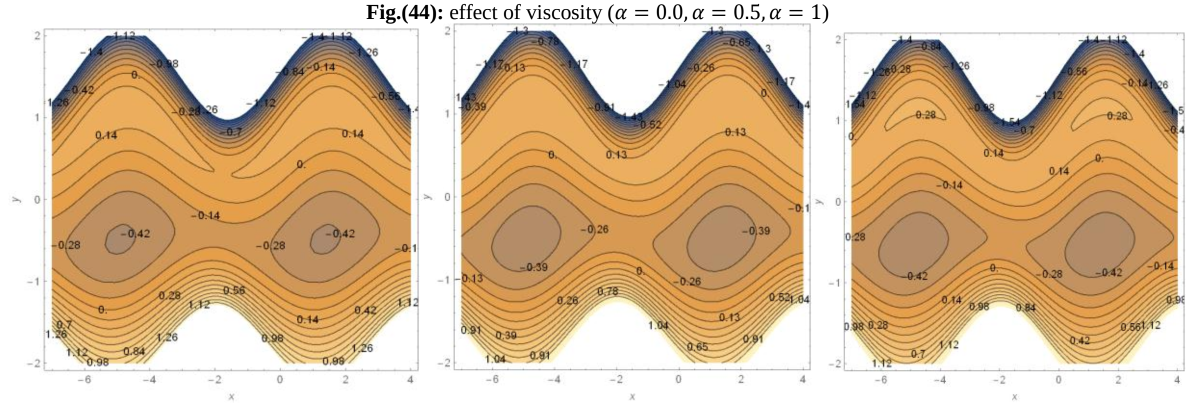

Fig.(45): effect of $\mathrm{F0} = 0.1, \mathrm{F0} = 0.2, \mathrm{F0} = 0.3$

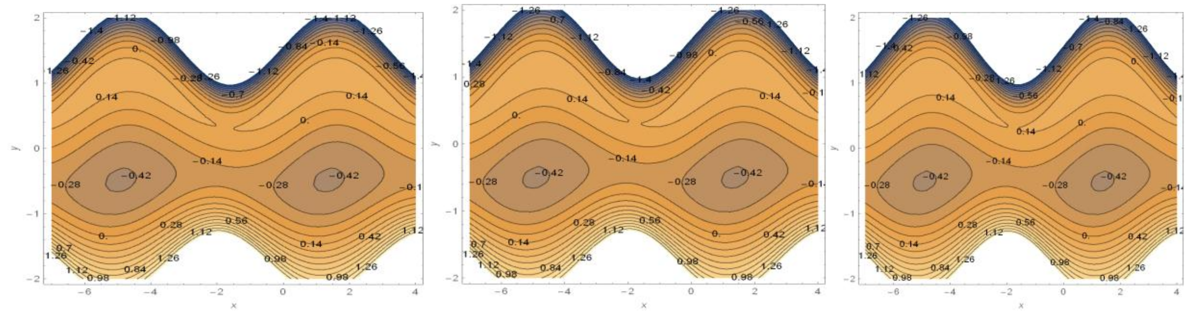

Fig.(46): effect of $k = 1, k = 2, k = 3$

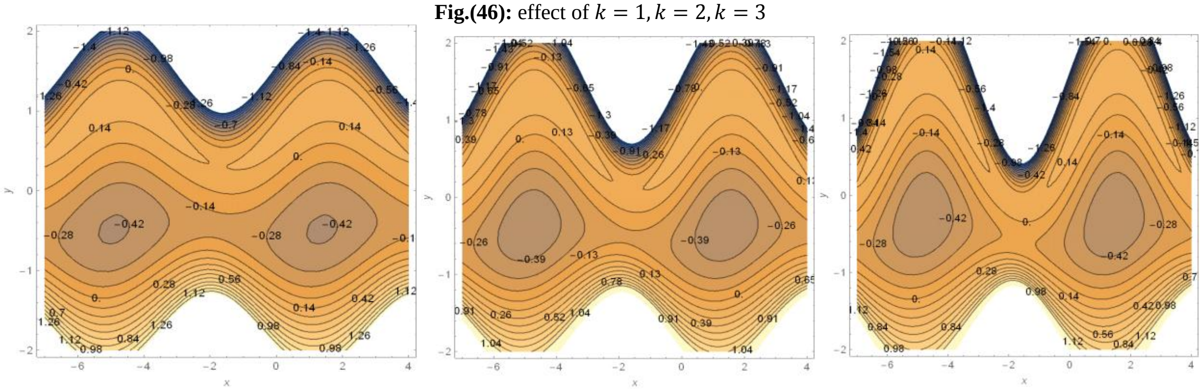

Fig.(47): effect of wall damping parameter r_1

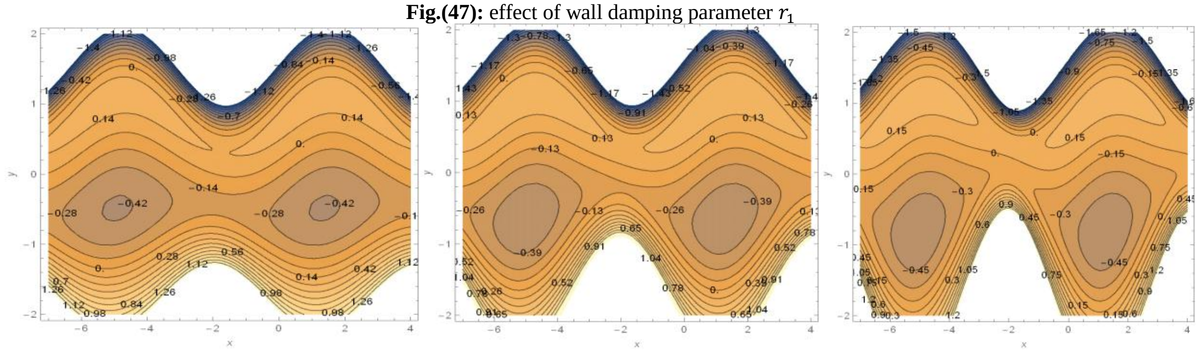

Fig.(48): effect of wall damping parameter r_2

6. CONCLUDING REMARK:

The present study deals with the combined effects of a magnetic field on peristaltic transport of Bingham plastic fluid.

1- The pressure gradient $\frac{dp}{dx}$ increases in magnitude with an increase of thermal conductivity (k) and decreases with an increase of the Hartman number M, F_0, and the second wall damping coefficient , in companion the impact of the other partient parameters is oscillatory or wobbling.
2- The pressure rise per wave length against θ increases in the pumping with an increase in thermal conductivity.
3- The pressure rise per wave length against θ decreases in the pumping with an increase in viscosity (α) and the Hartman number M.
4- The pressure rise per wave length against θ increases in the pumping $\theta < 0$ and decreases in the pumping $\theta > 0$ with an increase in phase difference ϕ.
5- The pressure rise per wave length against θ decrease in the pumping $x < 0$ and it is conversely in the pumping $x > 0$ with an increase of $r1,\ r2$.
6- The relationship between Δp and mean flow rate θ is linear with an increase of k.
7- The relationship between Δp and mean flow rate θ is nonlinear with an increase of M.
8- At the central region of the channel the axial velocity increases with an increase of $\phi, \alpha, r1, r2$ and decreases with an increase of F_0.
9- The axial velocity rise up at the upper wall with an increase of α and is conversely at the lower wall.
10- The axial velocity is oscillating with an increase of $M, F_0, k, r1$.
11- The profiles of velocity are parabolic.
12- The size of trapped bolus increases with an increase of $\alpha, F_0, r1, r2$, and decreases with an increase of ϕ, M.
13- The size and the number of trapped bolus increase with an increase of $\alpha, F_0, r1, r2$, and decrease with an increase of ϕ, M.
14- There are some points of deviation that change the flow of the fluid and its temperature can be change

with an increase of ϕ by clear way at the lower wall of the channel.

15- The temperature profile increases with an increase of the following parameters $\alpha, M, F_0, Br, Pr, r1, r2, Du, Sr, Sc$ and decreases with an increase of $v2$.

16- Temperature profiles increase with an increase of Bn at the beginning of the channel and decrease at the end of the channel.

17- The profiles of temperature and concentration distribution are parabolic in all figures.

18- The concentration distribution decreases with an increase of Sr, Sc. Opposite behavior for concentration distribution is noted when compared with temperature.

19- The concentration decreases with an increase of $\alpha, M, F_0, Br, Bn, Pr, r1, r2, Du, Sr, Sc$. It follows that the concentration is a decreasing function.

REFERENCES

1- Mokhtar Abd Elnaby, Mohamed H.Haroun. A new model for study the effect of wall properties on peristaltic transport of a viscous fluid. *Communications in Nonlinear Science and Numerical Simulation.* **Volume 13**, Issue 4, July 2008, Pages 752-762.

2- Misery AME, Hakeem AE, Naby AE, Nagar AHE. Effects of a fluid with variable viscosity and an endoscope on peristaltic motion. *Journal of the Physical Society of Japan* .**72(1)** · January 2003.

3- Ali N, Hussain Q, Hayat T, Asghar S. Slip effects on the peristaltic transport of MHD fluid with variable viscosity. *Physics Letters A.* **Volume 372**, Issue 9, 25 February 2008, Pages 1477-1489.

4- Akram S, Nadeem S, Hussain A. Effects of heat and mass transfer on peristaltic flow of a Bingham fluid in the presence of inclined magnetic field and channel with different wave forms. *Journal of Magnetism and Magnetic Materials.* **Volume 362**, August 2014, Pages 184-192.

5- Walton IC, Bittleston SH. The axial flow of a Bingham plastic in a narrow eccentric annulus. *Journal of fluid mechanics.* **Volume 222**, January 1991, pp. 39-60.

6- Javed M, Hayat T, Mustafa M, Ahmad B. Velocity and thermal slip effects on peristaltic motion of Walters-B fluid. *International Journal of Heat and Mass Transfer*.**Volume 96**, May 2016, Pages 210-217.

7- Khabazi NP, Taghavi SM, Sadeghy K. Peristaltic flow of Bingham fluids at large Reynolds numbers: A numerical study.*Journal of NonNewtonian Fluid Mechanics* .**Volume 227**, January 2016, Pages 30-44.

8- A.M.Abd-Alla,,S.M.Abo-Dahab and A.Kilicman, Peristaltic flow of a Jeffrey fluid under the effect of radially varying magnetic field in a tube with an endoscope. *J. Magn. Magn.Mater*. **384** (2015) 79-86.

9- A.M. Abd-Alla, S. M. Abo-Dahab and H.D.El-Shahrany, Effects of rotation and initial stress on peristaltic transport of fourth grade fluid with heat transfer and induced magnetic field, *J. Magn. Mat.* **349** (2014) 268-280.

10- K. Nowar, Peristaltic flow of a nanofluid under the effect of Hall current and porous medium, *Math. Prob. Eng.* **(4):15**, (2014).

11- M. Kothandapani and J. Prakash, Effect of radiation and magnetic field on peristaltic transport of nanofluids through a porous space in a tapered asymmetric channel. *J.Magn. Magn. Mater*. **378** (2015) 152-163.

12- T..Hayat ,S.Farooq, M Mustafa, B.Ahmad. Peristaltic transport of Bingham plastic fluid considering magnetic field, Soret and Dufore effect. *Results in physics* **7(**2017)2000-2011.

13- F.Alaa,A, M.Abdul Hadi. The effect of magnetic field on peristaltic transport of Bingham plastic fluid. *Jour of Adv Research in Dynamical &Control systems.***Vol(10**)10-special Issue 2018.